# Electrochemical determination of acrylate bone adhesive permeability during *in vitro* ageing and its predictive correlation with adhesive joint strength failure

Raja, M.[1], Shelton, J.C.[1], Salamat-Zadeh, F.[2], Tavakoli, M.[3], Donell, S.[4]., Watts, G.[5], and Vadgama, P.[1]

[1] *School of Materials and Engineering Science, Queen Mary University of London, Mile End Road, London, E1 4NS*
[2] *TWI, Granta Park, Great Abington, Cambridge, CB21 6AL*
[3] *KTN LTD, Suite 220 Business Design Centre, 52 Upper Street, London N1 0QH*
[4] *University of East Anglia, Norwich Research Park, Norwich, Norfolk NR4 7TJ*
[5] *Liverpool John Moores University, Byrom Street, Liverpool, L3 3AF*

*Correspondence:* m.a.a.raja@qmul.ac.uk

**Abstract**

This study assessed the solute permeability of a family of UV and moisture cured acrylates-based adhesives during *in vitro* ageing in pH 7.4 buffer. Acrylates have a potential role in bone fracture fixation, but their inability to allow microsolute exchange between the fractured bone surfaces may be important for effective healing. Cyclic voltammetry and chronoamperometry were used to determine diffusion coefficients for various electrochemically active probe molecules ($O_2$, $H_2O_2$, acetaminophen, catechol, uric acid and ascorbic acid) utilising proprietary acrylic, urethane – acrylate and cyanoacrylate adhesives. All adhesives proved to be impermeable for up to 9 days, following which a near-exponential increase in permeability resulted for all solutes. Diffusion coefficients at 18 days were in the range of $10^{-5}$ $cm^2s^{-1}$ and $10^{-6}$ $cm^2s^{-1}$ for $O_2$ and $H_2O_2$ respectively and $10^{-6}$ $cm^2s^{-1}$ for the organic solutes; no transport selectivity was seen for the latter. Adhesive joint strength showed a direct, inverse correlation with permeability and the more hydrophilic cyanoacrylates showed the greatest loss of strength. Adhesive permeabilisation does not appear to be compatible with the retention of bonding strength, but it can serve as a non-destructive surrogate for predicting mechanical strength changes during ageing.

***Key words****: adhesive, acrylates, diffusion coefficient, bone fracture, shear testing, tensile testing, hydration, ageing*

**List of Abbreviations**

CA – Cyanoacrylate

AU – Acrylate-Urethane

CV – Cyclic Voltammetry

PBS – Phosphate-Buffered Saline

MW – Molecular weight

DM – Dialysis Membrane

AM – Adhesive Membrane

DC – Diffusion Coefficient

## 1. Introduction

Bone fractures are a major cause of disability and present substantial pressures on health care services. In the US alone, there are an estimated 1.5 million fracture cases per annum leading to health costs of $17bn and with more active lifestyles, these figures are projected to increase by 50% in 2040 [1]. Standard fixation of fractures using metal plates and screws ensure stable positioning for bone healing and are particularly suited to fractures of major long bones. Even though this method provides stable, rigid fixation [2] the ancillary need for pins and screws can lead to complications of extrusion, migration and bone growth restriction [3]. Moreover, screw fixations require invasive drilling and necessitate strong and healthy bone around the fracture site. Where the bone is thin, weak or fragmented, further drilling can lead to added trauma and bone weakening, and further fracture a possibility [4, 5]. Screws can also lead to a focussing of stress loads promoting fixation failure [5]. Adhesives are an attractive alternative as potentially injectable, conformal bonding agents that do not necessitate further invasive procedures.

There is ongoing development of polymer-based adhesives for bone fixation, specifically, adhesives that undergo rapid *in vivo* setting, minimizing open surgical intervention and the associated extended inpatient stay. However, these adhesive have not to date provided the mechanical strength needed for weight bearing bones [6]. Following application, ideally, an adhesive is resorbed to allow for complete biological bridging by repair hard tissue (callus), however, well before this, there is a need for solute permeability to enable biological communication between fracture surfaces. Tissue remodelling, generally, requires active molecular signalling and solute cue mediated by cytokine and small molecule gradients and concentrations [7, 8]. Yet despite this biological imperative and the inevitable constraint a polymer barrier places on connective tissue communication, including bone, there has been no study characterising the permeability of medical adhesives. More generally, permeability will be a function of porosity, and if extended to the surface, this in turn will determine the completeness of the contact interface with the underlying bonded material. Such a microscopic property, moreover, will reflect on a key macro-scale property namely adhesive strength. The added complexity in this application is the unknown of the degradation – permeability link. All adhesives will age and/or degrade in water, and the rate of this has both implications for adhesion lifetime and progress towards increased permeabilisation. There is a tension between the demand for a stable adhesive and one that increases porosity over time for improved biological communication. It is well known that hydration leads to acrylate adhesive

degradation in water or moisture [9, 10], but the permeability correlation with strength has not been previously considered.

This study focuses on the early dry to wet stage permeability changes in an *in vitro* model using acrylate adhesives, an adhesive group of considerable medical interest for soft tissue bonding. A subset of this, namely cyanoacrylates, have been previously extensively studied [5], and their potential recognized in the 1950s, with a commercial product (Eastman 910®) emerging in 1958. Their suitability is partly based on low viscosity so penetration of voids and cavities in adherends is facilitated [11] and partly on structural versatility through functional side groups. They are appropriate for bone, as this is an example of a material with surface voids, and their variation through side chain modification allows for tailoring of strength and degradation. Longer side chains provide for higher strength and slower degradation [12-15], for example, butyl-cyanoacrylates have longer term strength than ethyl-cyanoacrylates [16-18] and degrade less quickly than methyl-cyanoacrylates [19].

Whilst acrylates can retain biomechanical strength under wet conditions [5], the toxicity of degradation products is a concern. Hydrolysis in buffer generates formaldehyde and cyanoacetate [20, 21], although during *in vivo* deployment, esterases lead to the generation of lower toxicity alcohol and poly(cyano acrylic) acid [15, 22, 23]. There are also individual variations; isobutyl 2-cyanoacrylate has proven to be non-toxic [24], whilst butyl-2-cyanoacrylate promotes tissue inflammation [25] and short chain cyanoacrylate is cytotoxic [26, 27].

At the extreme, complete surface sealing by an adhesive will retard bone repair [4], highlighting the need for tissue solute exchanges. Two adhesives types were considered; acrylate groups ($CH_2$=$CHCOO^-$) in acrylic and urethane-acrylate adhesives undergo free radical polymerisation under UV in the presence of photoinitiator, and cyanoacrylates (CAs) undergo anionic polymerisation in moisture facilitated by electron withdrawing –$COOCH_3$ and –CN groups [31, 32]. As adhesives are known to hydrate in water, an underlying aim was to understand the importance of water ingress [33]. The 'dry to wet' conversion is known to lead to strength loss and ultimately adhesive failure and the penetration of water is also known to lead to swelling and stresses within the interlocking surfaces [36, 37], reducing the efficacy of the adhesive prior to permeability changes and strength degradation, independent of any porosity increase. Use of permeability changes, utilizing a combination of cyclic voltammetry [28] and chronoamperometry [29, 30] thereby might allow tracking of adhesive strength change without the need for more complex and destructive mechanical testing.

We proposed to study the nature of the partial sealing imposed by degrading acrylate adhesives during ageing, which has not been considered in previosul studies. Permeability was calculated using two electroanalytical techniques; cyclic voltammetry and chronoamperometry. For cyclic voltammetry, peak current was used to obtain diffusion coefficients through the Randles-Sevcik equation:

$$i_p=\left(2.686\times10^5\right)n^{3/2}v^{1/2}D^{1/2}AC \qquad (1)$$

Where $i_p$ is peak current, n is the number of electrons, v is the scan rate, D is diffusion coefficient, A is electrode surface area and C is solute bulk concentration [38-43]. The second approach utilising chronoamperometry used transient, dynamic electrode responses to step changes in target molecule bulk solution concentration. This was monitored and matched on a real time basis against model simulated responses incorporating Fick's Laws. We have previously reported the use of a simplified software to achieve an accurate, bipartite solution to Fick's Laws that combines speed and repeatability [30, 44-49].

## 2. Experimental Details

### 2.1 Materials and Reagents

Di-sodium hydrogen phosphate ($Na_2HPO_4$), sodium dihydrogen phosphate ($NaH_2PO_4$), sodium chloride (NaCl) and sodium hydroxide solution (NaOH), were supplied by BDH (Dorset, UK). Deionised water was used for solution preparation and contact angle measurements. All experimental reagents; acetaminophen (analytical standard), l-ascorbic acid (reagent grade, crystalline), pyrocatechol (≥99%), hydrogen peroxide solution (30 wt. % in H2O, ACS reagent), and uric acid (≥99%, crystalline) were obtained from Sigma-Aldrich (Dorset, England).

All measurements were undertaken in phosphate buffer (PBS, 0.1 M, pH 7.4). Various stock solutions of 500 mM and 10 mM of the analytes, acetaminophen, l-ascorbic acid, pyrocatechol, hydrogen peroxide solution, and uric acid, were prepared in 0.1 M PBS and stored at 5°C.

For oxygen sensing, 50 ml of 0.1 M PBS was purged with nitrogen ($N_2$) gas to fully deoxygenate the solution and internal electrolyte film of the adhesive membrane covered electrodes. The deoxygenated solution was sealed with Parafilm® and stored at 5°C prior to use. For the diffusion studies, a separate 50 ml of 0.1 M PBS solution was air equilibrated and injected into the deoxygenated solution, which had been purged with nitrogen bubbling.

Cellulose dialysis tube membrane of flat width 76 mm was obtained from Sigma-Aldrich (Dorset, England). Glass microscope slides (75 x 50mm, Corning®, USA) were used to cast adhesive films. To

create fixed depth adhesive layers, 50µm diameter wire from an iPhone charger (Apple Inc. USA) was used as spacer. Platinum wires with porous Teflon tips (CH Instruments Inc., USA) were utilised as counter electrodes. Parafilm® (Bemis, USA) and Sellotape Original Tape (Henkel) were used to seal open vessels.

Proprietary medical grade acrylate adhesives (both moisture and UV curable) were supplied by Henkel (Hemel Hempstead, UK) (Table 1).

| Chemical Type | Cure Method / Trade Name | Reported Monomers |
|---|---|---|
| **Acrylate-Urethane** | UV Cure: Loctite 3301 | Isobornyl Acrylate<br>2-Hydroxyethyl acrylate<br>Urethane-acrylate oligomer (Proprietary) |
| **Acrylic** | UV Cure: Loctite 3926 | Isobornyl Acrylate<br>2-Hydroxyethyl acrylate |
| **Cyanoacrylate** | Moisture Cure: Loctite 4011,<br>UV Cure: Loctite 4304 | Ethyl 2-Cyanoacrylate |

Table 1: Adhesives used along with their known monomers

### 2.2 Strength Characterisation

Bone diaphyses from bovine metacarpus were thoroughly cleaned, cut along their longitudinal axes into rectangular geometries of lengths exceeding 8 x 8 x 23 mm. These rough-cut samples were ground utilising P60 - P800 (Klingspor Abrasives Inc., USA) papers and polished with P1000 - P4000 silicon carbide papers (Struers Ltd, UK) to obtain 5 x 5 x 20 mm cuboids. The samples were sonicated for 30 min, washed and stored at -20°C before use. For adhesive joint strength testing, adhesive was applied to bone overlap areas of 5 mm x 7 mm for lap shear and 5 mm x 5 mm for butt joint testing. Acrylate adhesive bond optimally at thicknesses of 1 mm, so adhesive depth was ensured by using spacer wires of 50 µm diameter. Moisture-cured adhesive was left for 24 hours at room temperature before testing. For UV curing, sequential 5 min UV exposure of each joint edge was carried out using an Omnicure Series 1500 light -curing lamp (EXFO Inc., Canada) and left for 24 hours before testing.

Adhesive joint strengths were determined with an Instron 5967 Dual Column Tabletop Universal Testing System (Instron, United States), with a cross-head speed of 0.5 mm/min.

### 2.3 Contact Angle Analysis

Adhesive was applied to glass microscope slides with a rocking motion to achieve uniform spread prior to curing. Contact angle measurements were carried out at room temperature using a deionised water drop applied *via* instrumented controlled needle flow on a Drop Shape Analyzer – DSA100 (KRÜSS GmbH, Germany) with a goniometer/image capture facility. Sessile drop fitting analysis was undertaken using the instrument program to establish contact angle of water drop. Ten readings were taken of each drop during first 5 seconds of drop application. Seven repeat measurements were taken for each contact angle value determination.

### 2.4 Electrochemical Measurements

A Rank Brothers inverted oxygen Electrode (Rank Brothers Ltd., UK) was used for electrochemical analysis. A PalmSens potentiostat (PalmSen, The Netherlands) was used for the voltammetry experiments. The potentiostat was software controlled using the PSTrace (PalmSen, The Netherlands) software package.

For adhesive membrane preparation of defined thickness, adhesive monomer was applied to a 75 - 80 mm length of dialysis membrane strip, and a second dialysis membrane was placed on top using two spacers (10 mm from each end). The laminate was allowed to cure (Section 2.2) whilst under compression between two microscope slides. A Leica Stereo Microscopes (Leica Microsystems, Germany) was used for cross sectional examination of the cured adhesive laminate

( 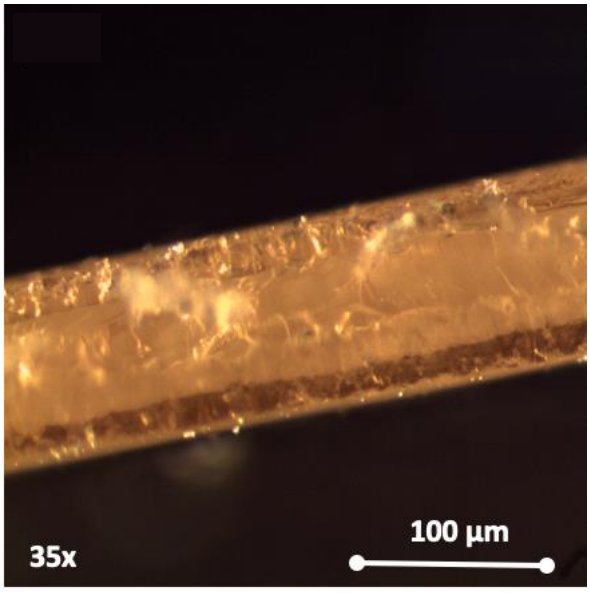


Figure 2). A laser micrometre (Mitutoyo, Hampshire, UK) was used for thickness measurements of the adhesive films.

Diffusion measurements of the target molecules were carried out with either a dialysis covered platinum electrode or with an electrode covered with a laminated tri-layer of dialysis membrane-adhesive-dialysis membrane. Membranes were pre-soaked in 0.1 M PBS solution for 10 minutes to ensure electrolyte loading into the dialysis membrane to serve as a bridging electrolyte between the Pt and Ag/AgCl reference electrode. The latter had the format of a partial ring round a Pt disc electrode and was set back from the plane of the working electrode (Figure 1). A platinum wire immersed in the solution above the Pt served as the counter electrode for CV studies. Assays used 5 ml PBS solution, and each CV based determination used 10 separate voltage sweeps.

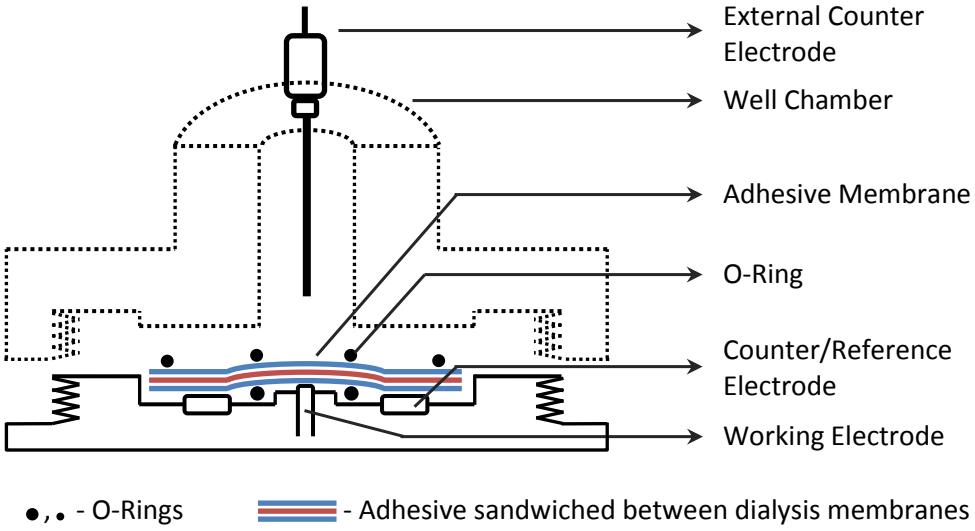


Figure 1: Schematic of cross-sectional view of the cell setup for modified electrode

For chronoamperometry, the cell set up was similar, except that the Ag/AgCl ring now served as a combined counter/reference electrode. A polarising voltage of +0.65V vs. Ag/AgCl was used for ascorbate, $H_2O_2$, acetaminophen, uric acid and catechol and of -0.65V vs. Ag/AgCl for oxygen. Three rapid syringe injections, 50 µl of 0.5 M analyte solution, were made in stirred solution to give concentration jumps in 5 mM steps. Air equilibrated buffer volumes were injected into de-oxygenated buffer for $O_2$ increments.

For the CV measurements, laminate covered electrodes were incubated for 70 min in assay solution to allow target molecule equilibration within the adhesive layer. This time interval was based on the maximum experimental time needed for completion of amperometric responses at these electrodes in the amperometric studies, to indicate the time needed for complete analyte penetration/partitioning.

**2.5 Ageing**

Adhesive joints and adhesive membranes were immersed in 100 mM phosphate buffered saline (pH 7.4) and stored in the Precision™ Compact Ovens at 37°C for 18 days. The joints and membranes were removed from the ovens every 3 days and tested for strength and permeability.

## 3. Results

### 3.1 Imaging

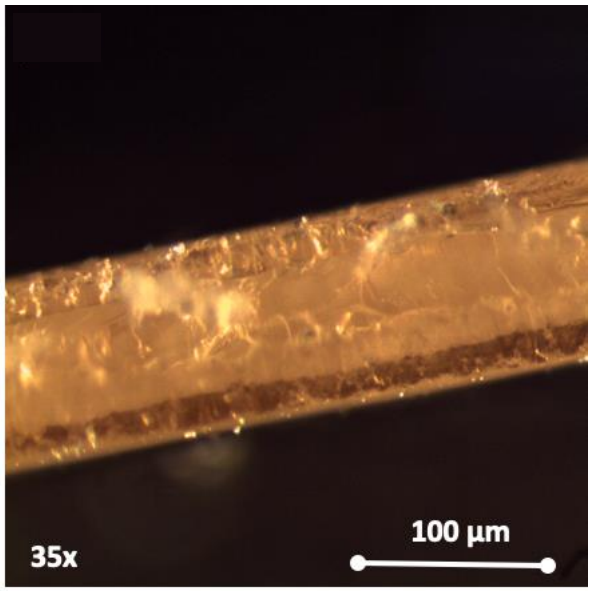


Figure 2: Stereomicroscopic cross section of adhesive layer laminate with dialysis membranes shown at higher magnification without galss slides

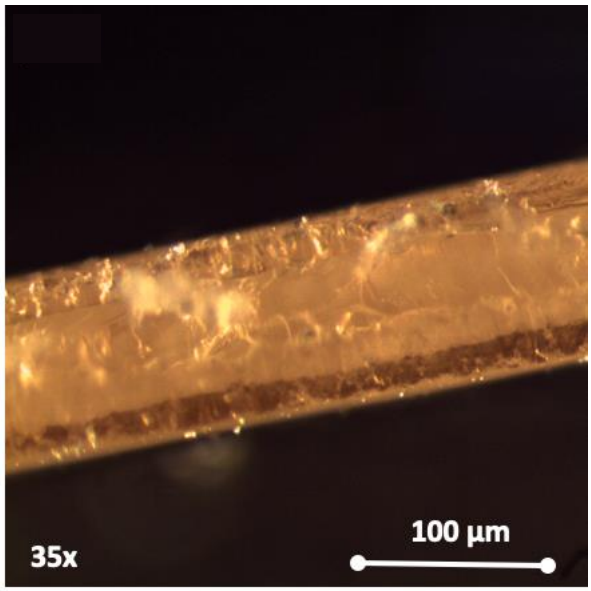


Figure 2 shows stereomicroscopic images of a cross section of adhesive layer laminates. The thickness of the adhesive membrane laminates was 100 ±0.004 µm. Dialysis membrane pieces were

used as permeable supporting structures for the adhesives. The molecular weight cut off (MWCO: 12,400) of these membranes was well above that of the test molecules, and initial permeability was established being at least an order of magnitude greater than that of the adhesive layers.

### 3.2 Contact Angle Measurement

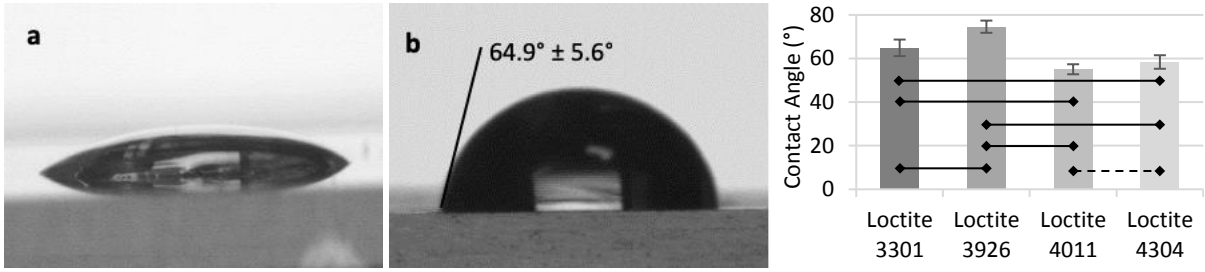


Figure 3: (a) Image of a flat UV cured Loctite 3301 surface before contact angle analysis, (b) Drop formation of deionised water on Loctite 3301 adhesive, and (c) Contact angle values formed for 4 propietary adhesives, namely acrylate urethane (Loctite 3301), acrylic (Loctite 3926); UV cure cyanoacrylate (Loctite 4011) and moisture cure cyanoacrylate (Loctite 4304). Solid lines represent presence of significant difference (Two Way ANOVA, $P<0.05$), whereas broken lines represent absence of significant difference (Two Way ANOVA, $P>0.05$), between two adhesives.

Figure 3 shows the contact angles recorded for drop formation of water on each adhesive. For cyanoacrylate (CA) adhesives, Loctite 4011 and Loctite 4304, there were no significant differences between contact angles. Loctite 3926, an acrylate only adhesive, showed the highest contact angle and was significantly different from the acrylate-urethane (AU) adhesive and the cyanoacrylate adhesives.

### 3.3 Electrochemical measurements

#### 3.3.1 Chronoamperometry

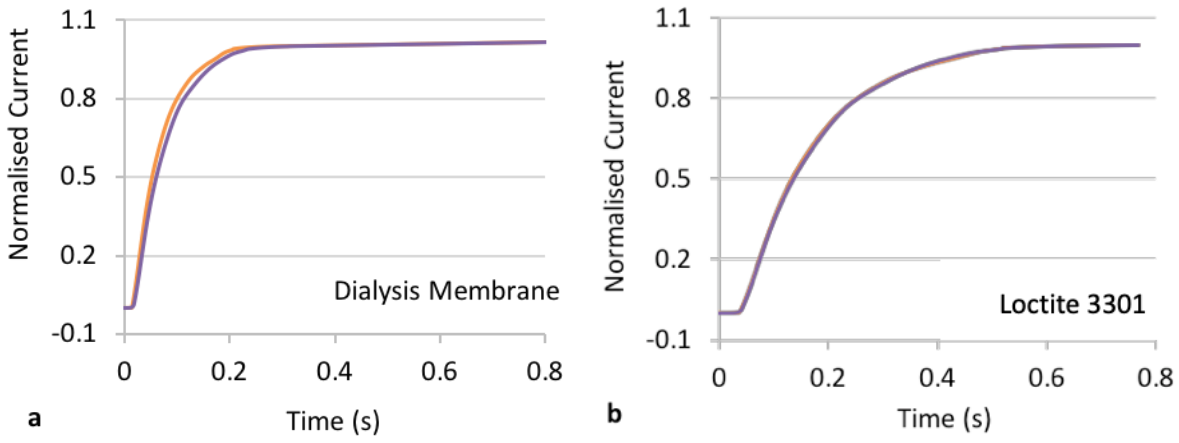

Figure 4: Example of experimental (■) and simulated (■) curves for hydrogen peroxide diffusion through (a) dialysis membrane (DM) and (b) Loctite 3301 adhesive membrane aged for 18 Days in Phosphate Buffer Solution (PBS, 0.1M, pH 7.4) at 37°C. Supporting electrolyte: PBS (100mM, pH 7.4).

The current-time profile provides an overall visual check on analyte diffusion and its consistency with a single rate-limiting Fickian diffusion barrier (Figure 4). Dialysis membrane (DM) covered electrodes displayed steep responses, signifying fast analyte diffusion through the DM and current stable steady state response under the stirring conditions and the sample volume used. Adhesive Membrane (AM) covered working electrodes on the other hand displayed slowly rising currents (Figure 5b), but again a steady state response, consistent with a higher diffusion barrier. The speed of response varied, however, depended partly on molecular weight (MW) with the much smaller oxygen and hydrogen peroxide, displaying steeper response prolifes than the organics; acetaminophen, ascorbic acid, catechol, and uric acid. Whilst with a DM covered electrode, current response was initiated immediately on analyte addition, AM covered electrodes showed a lag phase before registering a response; a response for organics was seen after 70 min on day 9 and after 20 min on day 18 upon addition to baseline solution. For oxygen/hydrogen peroxide response was triggered 40 min after addition on day 6 and in 10 min on day 18. This variation in response initiation also indicates a degree of size, but not charge, based permeation selectivity, and that it increases during ageing across the molecule range. Based on these findings, CV measurements were undertaken 70 min after electrode immersion in samples.

### 3.3.2 Cyclic Voltammetry

Preliminary diffusion studies with bare and dialysis membrane (DM) covered electrodes were conducted to establish baseline voltammograms.

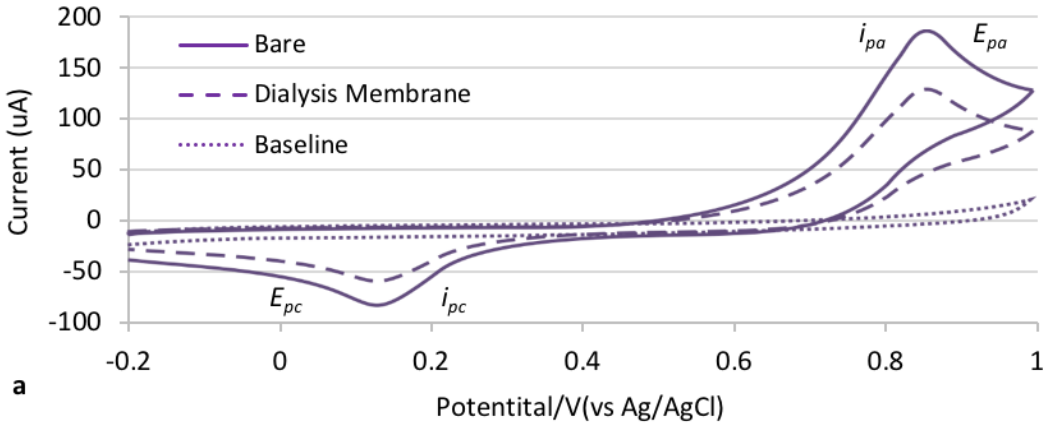

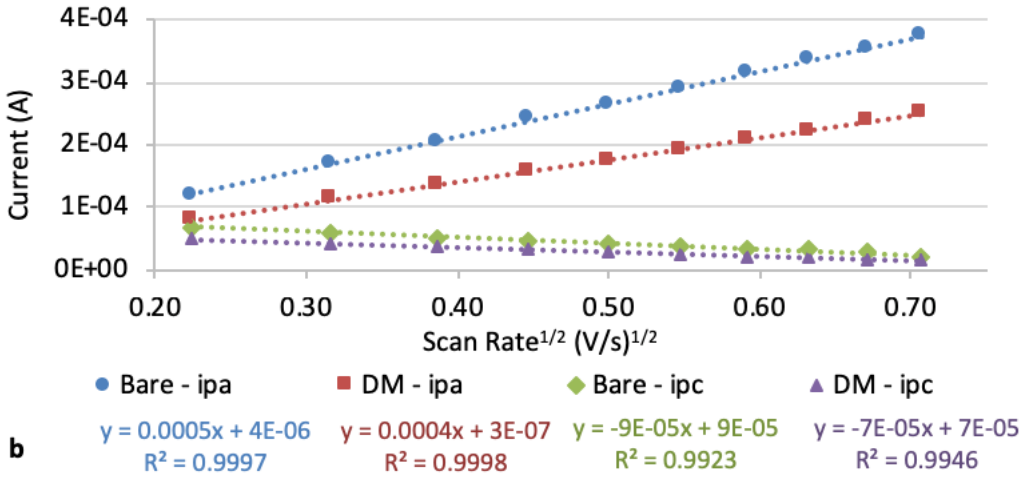


Figure 5: CVs of acetaminophen (10 mM in PBS) at 100mV/s vs Ag/AgCl showing (a) retained peak profile and (b) maintained diffusion control across a range of scan rates (100 – 500 mV/s) for a dialysis membrane covered Pt electrode.

The cyclic Voltammogram of acetaminophen (Figure 5) displayed reversible behaviour with defined anodic (oxidation) ($E_{pa}$= 0.85V) and cathodic (reduction) ($E_{pc}$= 0.13V) peak potentials, and corresponding redox peak currents $i_{pa}$ (0.17 mA) and $i_{pc}$ (0.09 mA). The observed peak separation potential ($\Delta E_p = E_{pa} - E_{pc}$) of 72 mV and the peak currents ratios ($|i_{pa}/i_{pc}| = 1.8$) is consistent with quasi-reversibility and electrochemical reduction followed by chemical reaction [50].

Acetaminophen displayed similar well-defined redox waves with dialysis covered and bare platinum electrodes. The peak potential and peak separation were identical which indicated that the dialysis membrane barrier had no effect on the electron transfer process (Yin et al., 2010). However, the peak currents were reduced; $i_{pa}$= 0.13 mA( $i_{pc}$= 0.06, $i_{pa}/i_{pc}| = 2.2$), confirming a barrier effect. The cyclic voltammograms for adhesive membrane (AM) covered electrodes showed a substantial decrease in peak current when compared to bare electrode signifying a major reduction in diffusivity of the electroactive species (Figure 6).

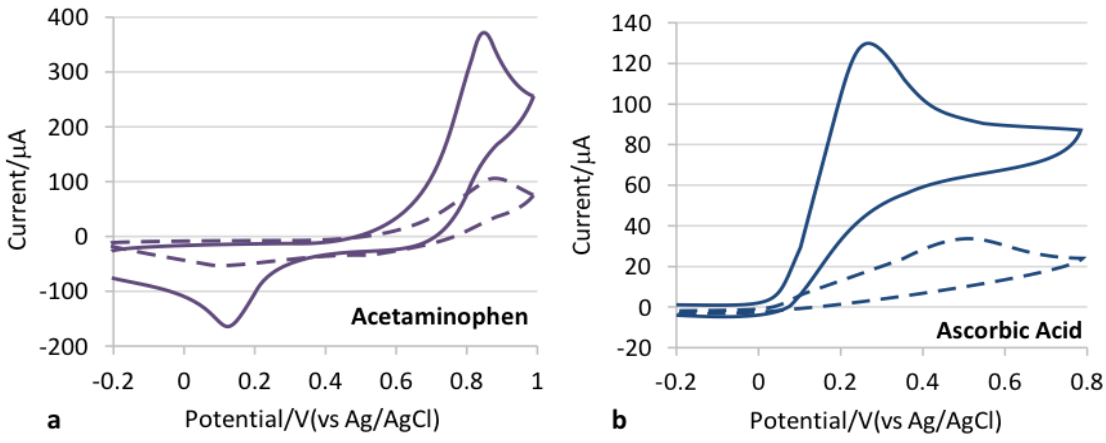

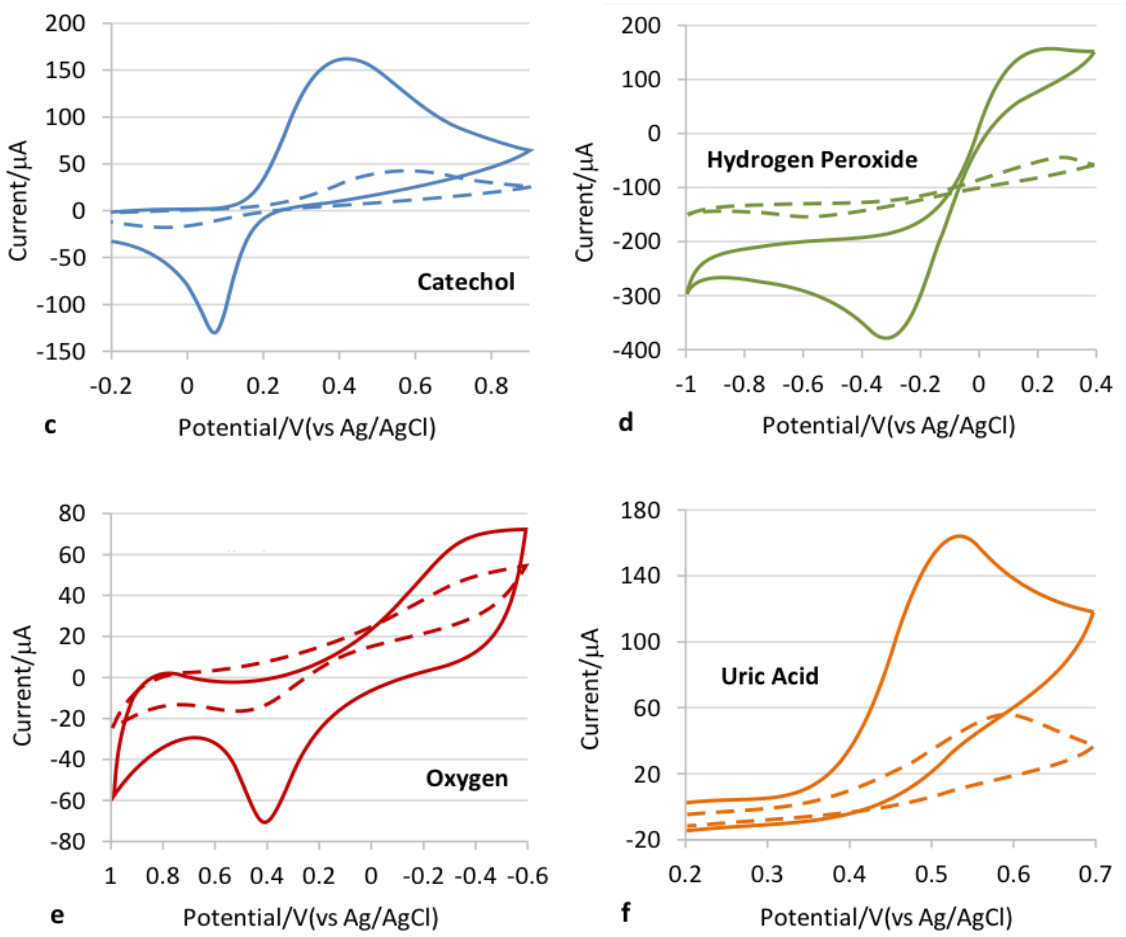


Figure 6: Day 15 cyclic voltammograms (broken lines) of various analytes diffusing through Loctite 3301 adhesive membrane aged in Phosphate Buffer Solution (0.1M, pH 7.4) at 37°C. Solid lines represent analytes diffusing through dialysis membrane. Scan rate: 100 mV/s.

Complete electrolyte conductivity was not achieved initially evident by a drifting baseline; this was only observed at day 6 which limited the period of use of CVs. The CVs for Loctite 3301 at day 15 presented in Figure 6 were similar in kind to those observed with the other adhesives. Considering the CVs, significant, measurable peaks were only demonstrated at day 9 when hydrogen peroxide and oxygen were used but extended to day 12 for the organics (Figure 7).

### 3.3.3 Diffusion Coefficients

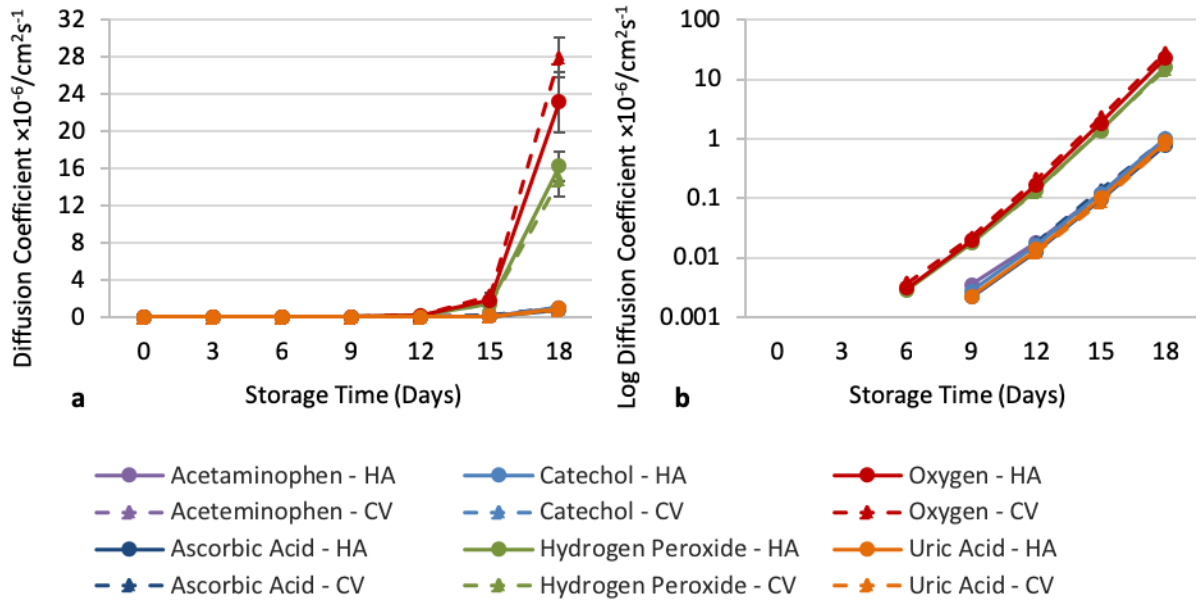


Figure 7: Diffusion coefficients obtained via cyclic voltammetry (CV) and chronoamperometry at various time periods during ageing for Loctite 3301 in PBS, 0.1M, pH 7.4 at 37°C. n =7

The pattern of change in permeability against time was similar for all adhesives and indicated a threshold effect of ageing with 9-12 days the time to open up the polymer pore structure. After this period, however, the permeability to all analytes increased in a logarithmic fashion for each diffusant and maintained the separation between the organic and non-organic groups, with a marginally, but significantly, greater transport rate for the non-polar oxygen compared with hydrogen peroxide (Fig 9). The consistency of these findings across the adhesive range for AA is shown in Fig 10.

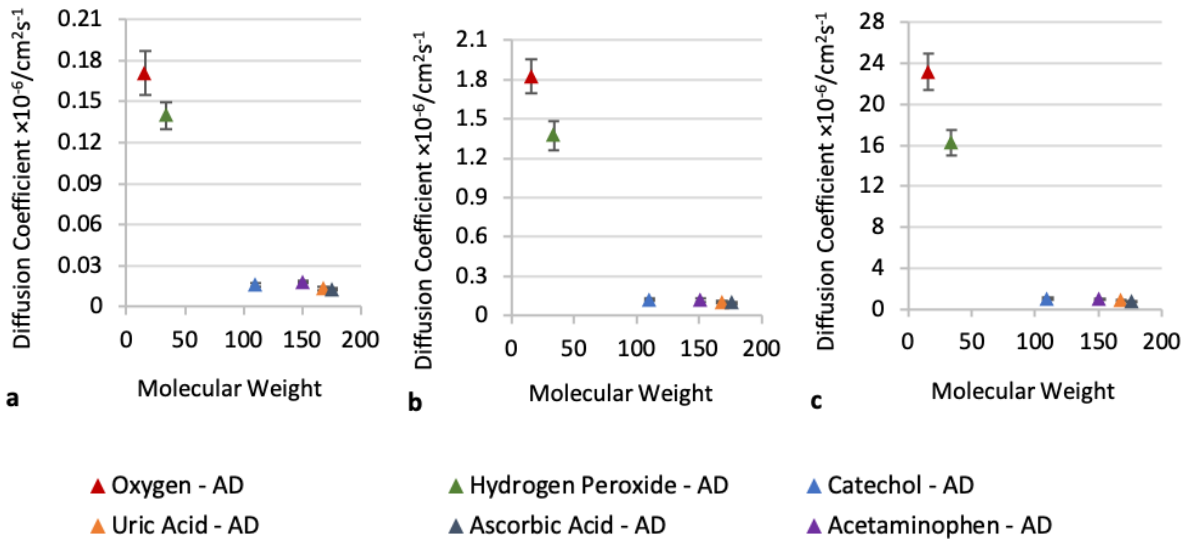

Figure 8: Diffusion coefficients of analytes *vs* molecular weight thorough a Loctite 3301 adhesive membranes at various time periods during ageing for Loctite 3301 in PBS, 0.1M, pH 7.4 at 37°C; (a) day 12, (b) day 15 (c) day 18.

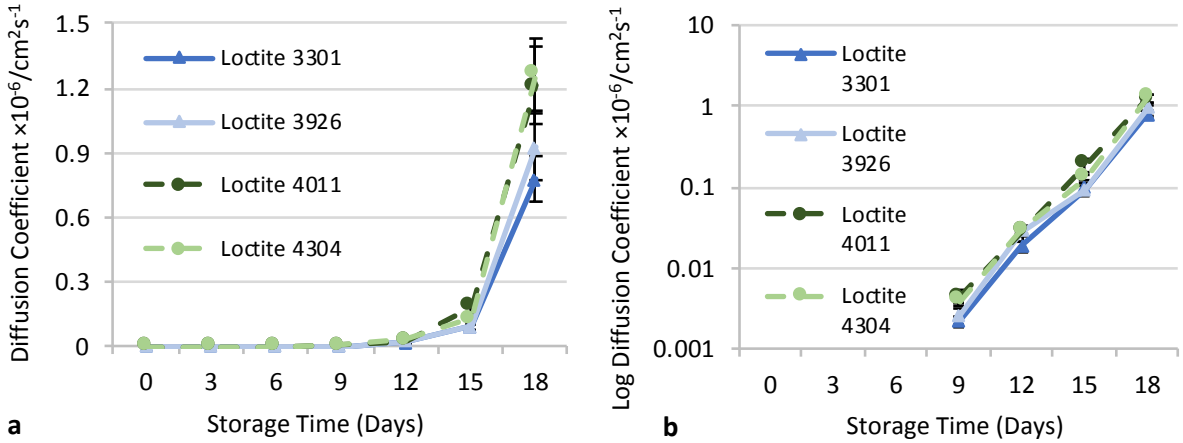


Figure 9: Diffusion coefficients (DC) of ascorbic acid following different storage periods for ascorbic acid through across the full range of adhesive polymers aged in PBS Solution, 0.1M, pH 7.4 at 37°C

Whilst the trends are similar, a consistent difference in permeability is seen between the different polymer types. However, notably, for the charged, diffusion through cyanoacrylate adhesive is faster than through acrylic and acrylate-urethane adhesives.

### 3.4 Strength measurement

Prior to any mechanical strength measurement were made, adhesive joint integrity was checked by fingertip pressure.

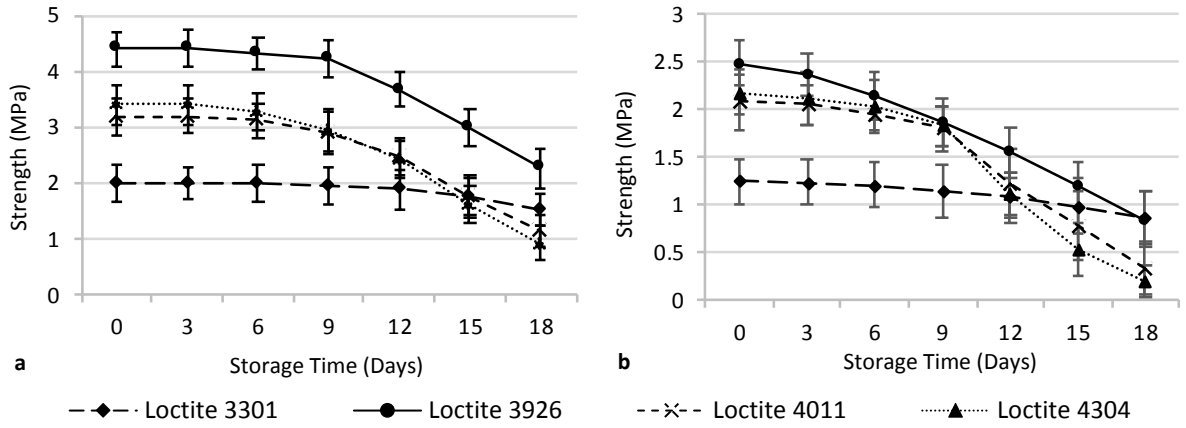


Figure 10: a) Single Joint Lap Shear Strengths and b) Tensile Butt Strengths of cyanoacrylate adhesives to bone after storage in PBS, 0.1M, pH 7.4 at 37°C for up to 18 days (n =7)

Figure 10 shows that butt joints were susceptible to ageing effects at an earlier stage than lap shear joints. The butt joints started to lose joint strength by day 6 compared to lap joints which retained

their initial strength up to at least day 9. In all cases, after the first loss in joint strength, the subsequent loss in strength was significant.

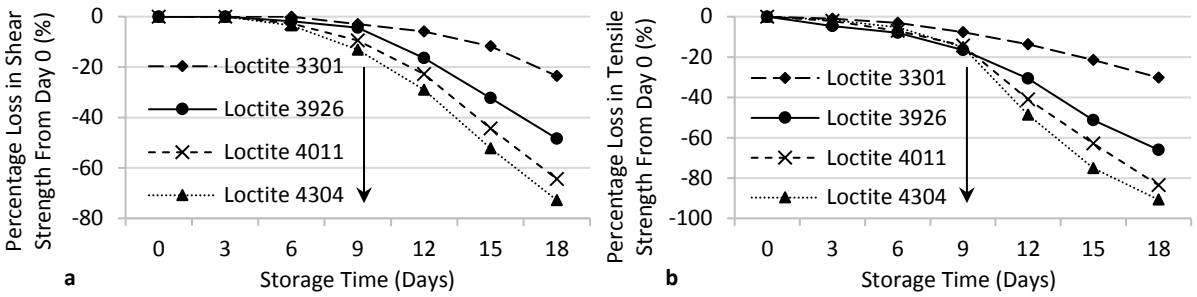


Figure 11: Percentage decrease, from day 0 of storage, for a) shear joint strength based on adhesive lap joints and b) tensile joint strength based on adhesive butt joints for adhesive polymers. Arrows represent decreasing contact angle (increasing hydrophilicity)

Figure 11 shows there was a hierarchy of strength loss dependent on increased surface hydrophilicity as indicated by contact angle.

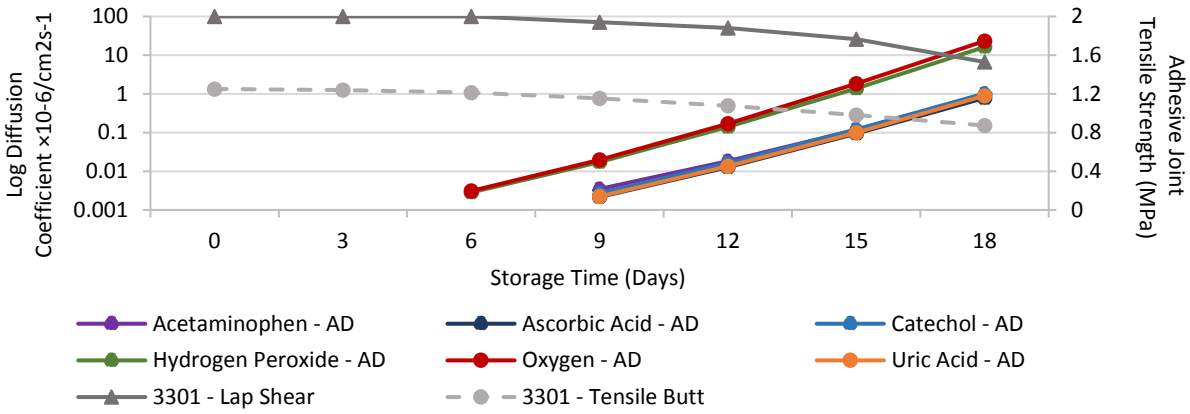


Figure 12: Plot of analyte permeability and Mechanical Strength (both Lap Shear and Tensile Butt) of aged acrylic urethane (**Loctite 3301**) adhesive

Figure 12 plots the decrease in adhesive joint strength and increase in adhesive permeability. In all instances, only once oxygen/hydrogen peroxide permeability was observable was a drop in strength detected. The organics provided a less sensitive alert of this.

## 4. Discussion

The absorption of water by polymers has been variously considered in terms of micro void uptake (*free volume theory*) and hydrogen bonding (*interaction theory*) [51-53]. The final steady state outcome is an equilibrium hydration state [54-56] defining general permeability behaviour. This is well recognised in the case of membrane based biosensors, where stable permeability and

selectivity is attained within minutes on exposure to a sample and which, in the absence of fouling, is relatively stable [57, 58]. The transport of water into polymers can permeabilise and indeed increase permeability exponentially [59], and this was observed in the adhesive polymers in the present study. It is possible, that for the dense adhesive layers, hydration equilibrium would have been slow, but a continued non-equilibration state extending beyond a week seems highly improbable for these relatively thin layers. So, the continued changes in permeability properties up to, and no-doubt, beyond the first 18 days of this study suggests that a degradation process occurring, although the creation of voids due to the release of leachables cannot be ruled out. What is unexpected is the lack of discrimination of organic probe molecules irrespective of charge, polarity or aromatic content (Figure 7). It appears that discrimination is on the basis of molecular weight with oxygen and hydrogen peroxide diffusing through faster. Agreement between the CV and amperometry data underpins the validity of the diffusion coefficient values. Further analysis of larger molecular weight species is required in order to determine higher molecular weight effects, but this is outside the scope of this study. The fact, also, that oxygen permeability provided the earliest indication of porosity change is further in line with the high tendency of all polymer barriers to allow gas transport [60] even if other solutes are blocked.

Along with an exponential increase in permeability, there was an even greater increase in small molecule transport. Although the first evidence of oxygen transport was at very low diffusion levels, it nevertheless provides a consistent indicator of the initiation of adhesive strength loss. This is a potentially useful titration point for evaluating the stage at which a candidate adhesive loses it adhesive strength and could be used for rapid screening of different materials. The rate of permeability increase during storage was also higher for the smaller molecules . Thus, on day 12, the $H_2O_2$:ascorbate diffusion coefficient ratio was 7:1, and by day 18 it was 15:1. This indicates a continued higher sensitivity when small molecules are tracked. The reason for the ratio change is unclear, however, but may reside in the opening up of smaller pores occurring at a later stage.

At the start of adhesive application, adhesive joint strength may be limited by arrested penetration into the bone pore structure due to progressive polymerisation. Viscosity will have a retarding effect on the rate of penetration, and therefore influenced its depth. During polymerisation, surface stresses resulting from polymer contraction may weaken adhesive-substrate bonding [61], but over time, the counter effect of water entry would lead to swelling and plasticisation thereby strengthening adhesive-substrate bonding through the swelling stress [36, 37]. None of this was seen in the present study, which again supports the notion of degradative change. If leachables were responsible for the greater permeability, then a loss of strength would not be expected.

Measured contact angles were of the order expected of polymeric surfaces, indicating mid-range hydrophobicity in all cases. There was difference between non-cyanoacrylate (Loctite 3301 and Loctite 3296) and cyanoacrylate (Loctite 4011 and Loctite 4304) adhesives, and a hydrophilicity trend was seen for different chemical types. Surface polarity decreased in the sequence: acrylic (Loctite 3296) < urethane-acrylate (Loctite 3301) < cyanoacrylate (Loctite 4011 and Loctite 4304). For cyanoacrylates, carbonyl (–C=O) and cyano (–C≡N) groups are known to increase polarity [31, 62-64] and their absence from acrylic adhesive will have led to higher hydrophobicity. Inclusion of urethane in the urethane-acrylates, however, will have introduced carbonyl groups [65, 66] leading to their hydrophilicity increase.

The generally accepted cut-off for wetting *vs* de-wetting by an adhesive is a 90° water contact angle [67]; all the present contact angles were below this value indicating a capacity for substrate penetration and wetting of hydrophilic surfaces which includes bone surfaces. Differences in polarity did not account for the initial strength difference (Figure 11)., which may have been the result of penetration differences due to the range of viscosities differeces of the adhesives. For practical purposes, laminates with polar dialysis membranes were readily made without delamination or variability in thickness; thicknesses of 100 ± 0.004 μm were consistently achieved. Polymer hydrophilicity did, however, have a bearing on the loss of mechanical integrity over time as the more hydrophilic a polymer the greater the loss of strength over time (Figure 11) with both shear and tensile strength showing a similar trend. Not only did the greater hydrophilicity lead to accelerated weakening but, notably, the same trend was seen for the increases in permeability.

There is clearly a direct correspondence between polymer porosity and adhesion strength, further underpinning the value of using the former as a surrogate of strength. Methodologically, CVs with membrane covered electrodes showed undistorted profiles giving linear $I_p$ *vs* $(V/s)^{½}$ plots across all scan rates, illustrated for acetaminophen (Figure 5). Amperometric responses, shown for hydrogen peroxide (Figure 4), also confirmed consistency with a simple diffusive Fickian model. There is a minor methodological advantage to using amperometry in that the electrode response profile can be compared with an ideal Fick's Law governed response. It is important to note however that the diffusion coefficients were measured and differences in partition coefficients across the polymers will have conditioned the actual flux of solute through the polymers. However, given that the solutes will have been transported through developing voids in the same adhesive polymer, it is unlikely that partition coefficients will have changed during ageing.

Comparability between permeability and adhesive joint strength cannot be expected, since the former is a bulk property whilst the latter is predominantly a surface phenomenon. The nature of

the substrate also adds further variables. Thus, bone, as a hydrophilic, porous, material is able to absorb water, and the trapped water may serves as a direct contact hydration source [68, 69], inevitably with maximal effect at the interface, and maximum effect on adhesive properties. Absolute strength values (Figure 10) show that shear joint strength loss is more steep than tensile joint strengths. This may reflect differences in adhesive layer geometry and the exposed surface area for water uptake. A greater water-exposed perimeter in the shear strength format led to the relative weakening or, alternatively, hydration from the bone substrate was more effective.

**4. Conclusion**

The joint strength of the adhesives examined was above the 0.2 MPa strength considered necessary for joint stabilisation [70]. Characterisation of ageing effects in this class of polymers is important, both in order to screen for effective adhesives allowing tissue molecular pathways and also to predict ageing outcomes *in vivo*. This is the first study to use permeability analysis as a bridge to mechanics; the finding of permeability initiation coinciding with joint weakening is an important indicator of hydration outcome. Molecular selectivity, as seen here for $O_2$ and $H_2O_2$, could be a basis for evaluating porosity using a further library of probe molecules, but also indicates that these as probe molecules provide the most sensitive index of mechanical degradation . Extension to large molecule studies will enable the stage at which cell signalling molecules can be transported across an adhesive joint, to be established. Such materials could also be used as drug release reservoirs to agents either accelerating bone growth or protecting from microbial biofilm formation. The limited microsolute diffusion seen here may have a beneficial role in bone regeneration.

*Acknowledgements* The authors wish to thank the EPSRC and TWI for generous support of the studentship for MR during this study and to Henkel for their donation of the adhesives.

**References**

[1] Bone Health and Osteoporosis: A Report of the Surgeon General, Rockville MD, 2004.
[2] T.P. Rüedi, W.M. Murphy, AO Principles of Fracture Management, in: C.L. Colton, A.F. Dell'Oca, U. Holz, J.F. Kellam, P.E. Ochsner (Eds.), Thieme, New York, 2000, pp. 864.
[3] W.E. Berryhill, F.L. Rimell, J. Ness, L. Marentette, S.J. Haines, Fate of rigid fixation in pediatric craniofacial surgery, Otolaryngology--Head and Neck Surgery, 121 (1999) 269-273.
[4] A. Nordberg, P. Antoni, M.I. Montanez, A. Hult, H. Von Holst, M. Malkoch, Highly adhesive phenolic compounds as interfacial primers for bone fracture fixations, ACS applied materials & interfaces, 2 (2010) 654-657.
[5] U. Kandalam, A.J. Bouvier, S.B. Casas, R.L. Smith, A.M. Gallego, J.K. Rothrock, J.Y. Thompson, C.Y. Huang, E.J. Stelnicki, Novel bone adhesives: a comparison of bond strengths in vitro, Int J Oral Maxillofac Surg, 42 (2013) 1054-1059.
[6] C. Heiss, N. Hahn, S. Wenisch, V. Alt, P. Pokinskyj, U. Horas, O. Kilian, R. Schnettler, The tissue response to an alkylene bis(dilactoyl)-methacrylate bone adhesive, Biomaterials, 26 (2005) 1389-1396.

[7] B. Behm, P. Babilas, M. Landthaler, S. Schreml, Cytokines, chemokines and growth factors in wound healing, Journal of the European Academy of Dermatology and Venereology, 26 (2012) 812-820.
[8] P. Niethammer, C. Grabher, A.T. Look, T.J. Mitchison, A tissue-scale gradient of hydrogen peroxide mediates rapid wound detection in zebrafish, Nature, 459 (2009) 996.
[9] A. Alghanem, G. Fernandes, M. Visser, R. Dziak, W.G. Renné, C. Sabatini, Biocompatibility and bond degradation of poly-acrylic acid coated copper iodide-adhesives, Dental Materials, 33 (2017) e336-e347.
[10] J.L. Cameron, S.C. Woodward, E.J. Pulaski, H.K. Sleeman, G. Brandes, R.K. Kulkarni, F. Leonard, The degradation of cyanoacrylate tissue adhesive. I, Surgery, 58 (1965) 424-430.
[11] S. Saska, E. Hochuli-Vieira, A. Minarelli-Gaspar, M.F.R. Gabrielli, M.V. Capela, M. Gabrielli, Fixation of autogenous bone grafts with ethyl-cyanoacrylate glue or titanium screws in the calvaria of rabbits, International journal of oral and maxillofacial surgery, 38 (2009) 180-186.
[12] J.V. Quinn, Tissue Adhesives in Clinical Medicine, BC Decker, Incorporated2005.
[13] J.C. Salamone, Concise Polymeric Materials Encyclopedia, Taylor & Francis1998.
[14] S. Dumitriu, Polymeric Biomaterials, Revised and Expanded, CRC Press2001.
[15] S.K. Bhatia, Biomaterials for Clinical Applications, Springer New York2010.
[16] M. Donkerwolcke, F. Burny, D. Muster, Tissues and bone adhesives—historical aspects, Biomaterials, 19 (1998) 1461-1466.
[17] D.F. Farrar, Bone adhesives for trauma surgery: A review of challenges and developments, International Journal of Adhesion and Adhesives, 33 (2012) 89-97.
[18] G.M. Brauer, J.W. Kumpula, D.J. Termini, K.M. Davidson, Durability of the bond between bone and various 2-cyanoacrylates in an aqueous environment, Journal of Biomedical Materials Research, 13 (1979) 593-606.
[19] J. Kilpikari, M. Lapinsuo, P. Tormala, H. Patiala, P. Rokkanen, Bonding strength of alkyl-2-cyanoacrylates to bone in vitro, J Biomed Mater Res, 20 (1986) 1095-1102.
[20] C. Evans, G. Lees, I. Trail, Cytotoxicity of cyanoacrylate adhesives to cultured tendon cells, Journal of Hand Surgery (British and European Volume), 24 (1999) 658-661.
[21] L. Montanaro, C.R. Arciola, E. Cenni, G. Ciapetti, F. Savioli, F. Filippini, L.A. Barsanti, Cytotoxicity, blood compatibility and antimicrobial activity of two cyanoacrylate glues for surgical use, Biomaterials, 22 (2000) 59-66.
[22] C. O'Sullivan, C. Birkinshaw, Hydrolysis of poly (n-butylcyanoacrylate) nanoparticles using esterase, Polymer degradation and stability, 78 (2002) 7-15.
[23] S. Dumitriu, V.I. Popa, Polymeric Biomaterials, CRC Press/Taylor & Francis2013.
[24] M.C. Harper, M. Ralston, Isobutyl 2-cyanoacrylate as an osseous adhesive in the repair of osteochondral fractures, Journal of Biomedical Materials Research Part A, 17 (1983) 167-177.
[25] M.A. Shermak, L. Wong, N. Inoue, B.J. Crain, M.J. Im, E.Y. Chao, P.N. Manson, Fixation of the craniofacial skeleton with butyl-2-cyanoacrylate and its effects on histotoxicity and healing, Plastic and reconstructive surgery, 102 (1998) 309-318.
[26] S.R. Mobley, J. Hilinski, D.M. Toriumi, Surgical tissue adhesives, Facial plastic surgery clinics of North America, 10 (2002) 147-154.
[27] S.C.d. Souza, C.H. Briglia, Comparative study of the use of ethyl cyanoacrylate adhesive and intracutaneous suture for cutaneous excision closure, Revista Brasileira de Cirurgia Plástica, 26 (2011) 566-572.
[28] F. Ismail, A. Willows, M. Khurana, P.E. Tomlins, S. James, S. Mikhalovsky, P. Vadgama, A test method to monitor in vitro storage and degradation effects on a skin substitute, Med Eng Phys, 30 (2008) 640-646.
[29] Z. Rong, P. Vadgama, Bipartite expressions for diffusional mass transport in biomembranes, Biophysical journal, 91 (2006) 4690-4696.

[30] Z. Rong, P. Vadgama, An electrochemical method for measurement of mass transport in polymer membranes using acetaminophen as a model system, Electrochimica acta, 54 (2009) 4949-4953.
[31] A. Pizzi, K.L. Mittal, Handbook of Adhesive Technology, Revised and Expanded, Taylor & Francis2003.
[32] T.Ç. Çanak, E. Kıraylar, İ.E. Serhatlı, Preparation and Application of Urethane Acrylate Coatings for Enhanching Mechanical Properties of Coagulated Surfaces, Karaelmas Science & Engineering Journal, 6 (2016).
[33] M. Unemori, Y. Matsuya, S. Matsuya, A. Akashi, A. Akamine, Water absorption of poly(methyl methacrylate) containing 4-methacryloxyethyl trimellitic anhydride, Biomaterials, 24 (2003) 1381-1387.
[34] H. Oysaed, I.E. Ruyter, Composites for use in posterior teeth: Mechanical properties tested under dry and wet conditions, Journal of Biomedical Materials Research, 20 (1986) 261-271.
[35] M.A. Cattani-Lorente, V. Dupuis, J. Payan, F. Moya, J.M. Meyer, Effect of water on the physical properties of resin-modified glass ionomer cements, Dental Materials, 15 (1999) 71-78.
[36] A.J. Feilzer, A.I. Kakaboura, A.J. de Gee, C.L. Davidson, The influence of water sorption on the development of setting shrinkage stress in traditional and resin-modified glass ionomer cements, Dental Materials, 11 (1995) 186-190.
[37] A.J. Feilzer, A.J. De Gee, C.L. Davidson, Curing contraction of composites and glass-ionomer cements, The Journal of prosthetic dentistry, 59 (1988) 297-300.
[38] F. Ismail, A. Willows, M. Khurana, P. Tomlins, S. James, S. Mikhalovsky, P. Vadgama, A test method to monitor in vitro storage and degradation effects on a skin substitute, Medical engineering & physics, 30 (2008) 640-646.
[39] S. Sambandam, J. Parrondo, V. Ramani, Estimation of electrode ionomer oxygen permeability and ionomer-phase oxygen transport resistance in polymer electrolyte fuel cells, Physical Chemistry Chemical Physics, 15 (2013) 14994-15002.
[40] A.J. Bard, L.R. Faulkner, Electrochemical Methods: Fundamentals and Applications, Wiley2000.
[41] X. Yuan, N. Xu, Determination of hydrogen diffusion coefficient in metal hydride electrode by cyclic voltammetry, Journal of Alloys and Compounds, 316 (2001) 113-117.
[42] X.H. Rui, N. Ding, J. Liu, C. Li, C.H. Chen, Analysis of the chemical diffusion coefficient of lithium ions in Li3V2(PO4)3 cathode material, Electrochimica Acta, 55 (2010) 2384-2390.
[43] N. Ding, J. Xu, Y.X. Yao, G. Wegner, X. Fang, C.H. Chen, I. Lieberwirth, Determination of the diffusion coefficient of lithium ions in nano-Si, Solid State Ionics, 180 (2009) 222-225.
[44] Z. Rong, S. Rashid, P. Vadgama, A Bipartite Expression for the Transient Amperometric Current at a Membrane Covered Planar Electrode to Characterize Solute Diffusion Through the Membrane, Electroanalysis, 18 (2006) 1703-1709.
[45] Z. Rong, P. Vadgama, Bipartite expressions for amperometric currents of recessed, membrane covered planar and hanging mercury drop electrodes, Journal of Electroanalytical Chemistry, 614 (2008) 166-170.
[46] A.T. Haug, R.E. White, Oxygen diffusion coefficient and solubility in a new proton exchange membrane, Journal of the Electrochemical Society, 147 (2000) 980-983.
[47] M.C. Kimble, R.E. White, Y.M. Tsou, R.N. Beaver, Estimation of the diffusion coefficient and solubility for a gas diffusing through a membrane, Journal of The Electrochemical Society, 137 (1990) 2510-2514.
[48] V. Compañ, M.A. Villar, E. Vallés, E. Riande, Permeability and diffusional studies on silicone polymer networks with controlled dangling chains, Polymer, 37 (1996) 101-107.
[49] J. Guzmán, M.T. Iglesias, E. Riande, V. Compañ, A. Andrio, Synthesis and polymerization of acrylic monomers with hydrophilic long side groups. Oxygen transport through water swollen membranes prepared from these polymers, Polymer, 38 (1997) 5227-5232.

[50] H. Filik, A.A. Avan, S. Aydar, G. Çetintaş, Determination of acetaminophen in the presence of ascorbic acid using a glassy carbon electrode modified with poly (caffeic acid), Int. J. Electrochem. Sci, 9 (2014) 148-160.
[51] S. Venz, B. Dickens, NIR-spectroscopic investigation of water sorption characteristics of dental resins and composites, Journal of biomedical materials research, 25 (1991) 1231-1248.
[52] N. Marcovich, M. Reboredo, M. Aranguren, Moisture diffusion in polyester–woodflour composites, Polymer, 40 (1999) 7313-7320.
[53] R.E. Kerby, L.A. Knobloch, S. Schricker, B. Gregg, Synthesis and evaluation of modified urethane dimethacrylate resins with reduced water sorption and solubility, Dental Materials, 25 (2009) 302-313.
[54] S. Deb, M. Braden, W. Bonfield, Water absorption characteristics of modified hydroxyapatite bone cements, Biomaterials, 16 (1995) 1095-1100.
[55] R.E. Shalin, Polymer Matrix Composites, Springer1995.
[56] I.D. Sideridou, M.M. Karabela, D.N. Bikiaris, Aging studies of light cured dimethacrylate-based dental resins and a resin composite in water or ethanol/water, Dental Materials, 23 (2007) 1142-1149.
[57] S. Anastasova, A.-M. Spehar-Délèze, D. Bickham, P. Uebel, M. Schmidt, P. Russell, P. Vadgama, Stabilised Biosensing Using Needle-Based Recess Electrodes, Electroanalysis, 24 (2012) 529-538.
[58] B. Yu, Y. Moussy, F. Moussy, Lifetime improvement of glucose biosensor by epoxy-enhanced PVC membrane, Electroanalysis: An International Journal Devoted to Fundamental and Practical Aspects of Electroanalysis, 17 (2005) 1771-1779.
[59] J. Siepmann, R.A. Siegel, M.J. Rathbone, Fundamentals and Applications of Controlled Release Drug Delivery, Springer2011.
[60] D.H. Kim, Y.S. Ryu, S.H. Kim, Improvements in the oxygen barrier property of polypropylene nanocomposites, Polymers for Advanced Technologies, (2018).
[61] L.F.M. da Silva, A. Öchsner, R.D. Adams, Handbook of Adhesion Technology, Springer Berlin Heidelberg2011.
[62] F.F. Fleming, L. Yao, P. Ravikumar, L. Funk, B.C. Shook, Nitrile-containing pharmaceuticals: efficacious roles of the nitrile pharmacophore, Journal of medicinal chemistry, 53 (2010) 7902-7917.
[63] G. Plopper, Principles of Cell Biology, Jones & Bartlett Learning2012.
[64] A. Attanasio, I.S. Bayer, R. Ruffilli, F. Ayadi, A. Athanassiou, Surprising High Hydrophobicity of Polymer Networks from Hydrophilic Components, ACS applied materials & interfaces, 5 (2013) 5717-5726.
[65] I. Sideridou, V. Tserki, G. Papanastasiou, Study of water sorption, solubility and modulus of elasticity of light-cured dimethacrylate-based dental resins, Biomaterials, 24 (2003) 655-665.
[66] V.D. Athawale, M.A. Kulkarni, Preparation and properties of urethane/acrylate composite by emulsion polymerization technique, Progress in Organic Coatings, 65 (2009) 392-400.
[67] Y. Yuan, T.R. Lee, Contact Angle and Wetting Properties, 51 (2013) 3-34.
[68] M. Bowditch, The durability of adhesive joints in the presence of water, International Journal of Adhesion and Adhesives, 16 (1996) 73-79.
[69] E.M. Knox, M.J. Cowling, Durability aspects of adhesively bonded thick adherend lap shear joints, International Journal of Adhesion and Adhesives, 20 (2000) 323-331.
[70] N.V. Shah, R. Meislin, Current State and Use of Biological Adhesives in Orthopedic Surgery, Orthopedics, 36 (2013) 945-956.